bioRxiv preprint doi: https://doi.org/10.1101/2023.03.09.531962; this version posted March 10, 2023. The copyright holder for this preprint (which was not certified by peer review) is the author/funder, who has granted bioRxiv a license to display the preprint in perpetuity. It is made available under aCC-BY 4.0 International license.

1 # Icariin prevents depression-like behaviors in chronic unpredictable mild stress-induced rats
2 through Bax/cytoplasm C/caspase-3 axis to alleviate neuronal apoptosis

3 Xiao Wu[1, #], Xiaona Zhang[2, #], Lulu Sun[2], Xiaomin Lu[1,*], Cunsi Shen[3,*]

4 [1]Department of Respiratory Medicine, Jiangsu Provincial Hospital of Chinese Medicine, Affiliated
5 Hospital of Nanjing University of Chinese Medicine, Nanjing, Jiangsu, 210000, China.

6 [2]Nanjing University of Chinese Medicine, Nanjing, Jiangsu, 210023, China.

7 [3]Jiangsu Key Laboratory of Pediatric Respiratory Disease, Affiliated Hospital of Nanjing University of
8 Chinese Medicine, Nanjing, Jiangsu, 210023, China.

9 [#]These authors contributed equally to this work.

10 ***Corresponding Author:**

11 Xiaomin Lu, Department of Respiratory Medicine, Jiangsu Provincial Hospital of Chinese Medicine,
12 Affiliated Hospital of Nanjing University of Chinese Medicine, No. 155 Hanzhong Road, Nanjing,
13 Jiangsu, 210000, China.E-mail:xmlu78@126.com

14 Cunsi Shen, Jiangsu Key Laboratory of Pediatric Respiratory Disease, Affiliated Hospital of Nanjing
15 University of Chinese Medicine, No. 155 Hanzhong Road, Nanjing, Jiangsu, 210023, China.

16 E-mail: shencunsi@163.com

17 **Author's E-mail:**

18

19 Xiaomin Lu:xmlu78@126.com
20 Xiao Wu:xxzjwx2010@126.com
21 Xiaona Zhang:ZXN2725381241@163.com
22 Lulu Sun:s366663@126.com
23

24

25 ## Abstract

26 Major depressive disorder (MDD) affects approximately 16% of the global population. Our previous
27 study has demonstrated that icariin (ICA) exhibits anti-depressant activity by increasing the expression

bioRxiv preprint doi: https://doi.org/10.1101/2023.03.09.531962; this version posted March 10, 2023. The copyright holder for this preprint (which was not certified by peer review) is the author/funder, who has granted bioRxiv a license to display the preprint in perpetuity. It is made available under aCC-BY 4.0 International license.

28 of Brain Derived Neurotrophic Factor (BDNF) in a rat model of chronic unpredictable mild stress
29 (CUMS). In this study, we investigated whether and how ICA can prevent CUMS-induced depression-
30 like behaviors in rats by modulating hippocampus neuronal apoptosis. Forty male rats were randomly
31 divided into control, CUMS, CUMS-fluoxetine (Flx) (10 mg/kg), and CUMS-ICA (20 mg/kg) groups.
32 Behavior tests including sucrose preference test (SPT), open field test (OFT), elevated plus-maze (EPM),
33 and forced swimming tests (FST) were performed. The Nissl staining and TUNNEL assay were used to
34 determine neuronal apoptosis. Subsequently, expression of glucocorticoid receptor (GR), Bcl-2,
35 cytochrome C, caspase-3 and Bax in the hippocampus were tested by western blot . Our results show that
36 a chronic administration of ICA (20 mg/kg) can prevent CUMS-induced depressant-like behaviors in
37 male model rats. Additionally, ICA significantly inhibited mitochondrial translocation of GR, reduced
38 mitochondrial outer membrane permeabilization (MOMP) to suppress the release of cytochrome C, and
39 then inhibit the activation of caspase-3. In conclusion, our research provides new evidence to understand
40 the anti-depressant activity of ICA, which relates to its inhibition of neuronal apoptosis in hippocampus
41 through mitochondrial apoptotic pathway.

42 **Key words** neuronal apoptosis, ICA, Bax, caspase-3, cytochrome C

43

44 Introduction

45 Stress, especially psychosocial stress, plays a crucial role in the pathogenesis of major depressive disorder
46 (MDD) [1]. Now, mental disorders account for a large proportion of the burden of disease in
47 governments around the world, surpassing cardiovascular and cancer diseases [2]. According to the
48 World Health Organization, depression will become the second leading cause of disability in 2030.
49 Although several antidepressants targeting the serotonin and/or norepinephrine systems have been used
50 to treat depression [3, 4]. There is still no evidence of a reduction in the population burden of depression.
51 One possible explanation is that treatment may not be adequately available, effectively available to have

bioRxiv preprint doi: https://doi.org/10.1101/2023.03.09.531962; this version posted March 10, 2023. The copyright holder for this preprint (which was not certified by peer review) is the author/funder, who has granted bioRxiv a license to display the preprint in perpetuity. It is made available under aCC-BY 4.0 International license.

52 an impact [5]. So, different strategies, such as preventive or alternative medicine, need to be further
53 explored [6].
54 The hippocampus is a vital component of brain, it participates in several important functions, including
55 behaviors, mental and intellectual activities, in both rodents and human [7] . Morphological changes in
56 brain tissues are observed with long-term MDD, in particular a decreased volume and neuronal apoptosis
57 of the hippocampus [8]. Physiologically, when the hypothalamus-pituitary-adrenal (HPA) axis is
58 activated, the adrenal glands secrete glucocorticoids (GCs). During chronic stress, dysfunction of the
59 HPA axis is accompanied by significant changes in neuroendocrine function. HPA axis activation can
60 be regulated by negative feedback mechanisms that activate glucocorticoid receptor (GR) at different
61 locations, including the hippocampus, prefrontal cortex (PFC) and upper brain structures [11], where
62 dissociated GR signals to the nucleus and regulates the target genes. Mitochondria are essential
63 organelles that regulate cellular homeostasis and cell survival [12]. More and more evidence suggests
64 that MDD may be a consequence of abnormal mitochondrial function [13]. Due to a vital role of in cell
65 physiology, mitochondria should be the first responder to stress. Animal studies have also shown that
66 CUMS inhibits mitochondrial oxidative phosphorylation, dissipates mitochondrial membrane potential,
67 and disrupts the mitochondrial ultrastructure of various brain regions, including mouse hippocampus,
68 cortex and hypothalamus [14]. For example, Rudranil De et al. revealed that Bax can act as the central
69 mediator by translocating into mitochondria and inducing neuronal apoptosis when brain tissue is
70 stimulated by stress [15]. In addition, mitochondrial transcription and energy metabolism are also
71 affected by GCs [16]. The effect of GCs on mitochondrial processes can be explained by GR translocation
72 to mitochondria [17]. The previously confirmed mitochondrial translocation of activated GR in DP
73 thymocytes provides an intriguing explanation for its marked sensitivity to GC-induced apoptosis [18].
74 However, the fine molecular details of how the mitochondrial translocation of GR regulates neuronal
75 apoptosis remained unclear.

bioRxiv preprint doi: https://doi.org/10.1101/2023.03.09.531962; this version posted March 10, 2023. The copyright holder for this preprint (which was not certified by peer review) is the author/funder, who has granted bioRxiv a license to display the preprint in perpetuity. It is made available under aCC-BY 4.0 International license.

76 Icariin (ICA) is a flavonoid glucoside isolated from *Epimedium brevicornu Maxim*, which is frequently
77 used in traditional Chinese medicine (TCM) to treat asthma [19], kidney disease [20], testicular
78 dysfunction [21] and cartilage damage [22]. TCM is often used to treat depression, for example,
79 paeoniflorin improves chronic stress-induced depression behavior in mice model by influencing the
80 ERK1/2 pathway [23]. Zhang et al. revealed that Xiaoyao powder can reduce the damage of hippocampal
81 neurons in CUMS-induced hippocampal depression model rats through connexin 43Cx43/GR/brain-
82 derived neurotrophic factor signaling pathway [24]. Classically, ICA has also been reported to exert
83 antidepressant-like actions. Our previous work showed that ICA improves hippocampal
84 neuroinflammation by inhibiting HMGB1-associated pro-inflammatory signals in LPS-induced
85 inflammatory models of C57BL/6 J mice [25]. In addition, ICA by inhibiting NF-κB signal activation
86 and NLRP3-inflammasome/caspase-1/IL-1β axis plays an antidepressant-like role in CUMS model of
87 depression in rats [26]. Otherwise, ICA reduces Glu-induced excitatory neurotoxicity through antioxidant
88 and anti-apoptotic pathways in SH-SY5Y cells [27]. However, whether ICA is beneficial for the
89 depression via ameliorating neuronal apoptosis in the hippocampus is still unknown.
90 In this study, the CUMS protocol was used as a rat model for depression, which mimicked many
91 symptoms of human depression [34]. Understanding the molecular regulatory mechanism of neuronal
92 apoptosis under the CUMS-induced depression-like behavior in rat model may provide the novel
93 therapeutic targets for depression. Therefore, the purpose of the present study was to identify the anti-
94 apoptosis mechanism of ICA in the hippocampus on the CUMS-induced depression-like behavior in
95 male rat model. In addition, GR, Bax, Bcl-2, Caspase 3, Cleaved Caspase 3, and cytochrome C levels in
96 the hippocampus were measured to explain the possible mechanism of ICA. Here, we provided evidence
97 for the activation of the mitochondrial apoptotic pathway associated with GR after ICA treatment in
98 hippocampus, which support ICA might act as an important drug in the prevention of depression.
99

bioRxiv preprint doi: https://doi.org/10.1101/2023.03.09.531962; this version posted March 10, 2023. The copyright holder for this preprint (which was not certified by peer review) is the author/funder, who has granted bioRxiv a license to display the preprint in perpetuity. It is made available under aCC-BY 4.0 International license.

100 **Methods and materials**

101 **Drugs and reagents**

102 ICA (the purity is 98.93%) was purchased from Shanghai Ronghe Medical Science Co., Ltd. (Shanghai,
103 China). Dimethyl sulfoxide (DMSO) was used to prepare ICA stock solutions and diluted with sterile
104 normal saline (DMSO concentration: 0.1%) [35]. Fluoxetine (Flx) was purchased from Eli Lilly and
105 Company (Suzhou, China) and diluted to 10 mg/mL with sterile saline solution [36]. Mitochondria
106 Isolation Kit for Tissue (No.89801) was bought from Thermo Fisher Scientific Inc. Rat corticosterone
107 (CORT) ELISA kits from ebioscience (San Diego, CA) were purchased from Beyotime Biotech Inc.,
108 China. Mouse anti-GR (1:1000), mouse anti-Bcl-2, mouse anti-Bax (1:400, Santa Cruz Biotechnology,
109 Santa Cruz, CA, USA), anti-β-actin, anti-Cox-IV, anti-caspase-3, cleaved caspase-3, anti-cytochrome C
110 (1:1000, Bioworld Technology Co., Ltd, Nanjing, China). Tunnel was bought from Wuhan Boster Co.,
111 Ltd. (China).

112

113 **Animals**

114 All experimental male Sprague-Dawley (SD) rats weighing 120-140 g (5 weeks old) were purchased
115 from Shanghai SLAC Co. (Shanghai, China). The animals were kept in temperature (20 ± 2 °C), humidity
116 (50–60%) and 12 h light/dark cycle (light period from 6:00 am to 18:00 pm) and free of food and water
117 *ad libitum*. To avoid fighting among male rats, prior to the experiment, all animals were maintained in a
118 single cage for at least seven days [37]. All experiments were conducted in accordance with the guidelines
119 of the Animal Care and Use Committee at Huashan Hospital of Fudan University. Make every effort to
120 reduce the suffering of animals. In addition, all procedures were approved by the Animal Care Ethics
121 Committee of Huashan Hospital of Fudan University (approval number: [HS-A-2021-0721]).

122

123 **Chronic Unpredictable Mild Stress (CUMS) procedure and drug treatments**

bioRxiv preprint doi: https://doi.org/10.1101/2023.03.09.531962; this version posted March 10, 2023. The copyright holder for this preprint (which was not certified by peer review) is the author/funder, who has granted bioRxiv a license to display the preprint in perpetuity. It is made available under aCC-BY 4.0 International license.

124 Forty rats were randomly divided into 4 groups (10 rats/group): Control, CUMS-vehicle, CUMS-Flx
125 (positive control, 10 mg/kg), and CUMS-ICA (20 mg/kg). Control group rats were grouped housed in a
126 separate room under standard conditions. All rats that underwent the CUMS procedure were single
127 housed. The CUMS procedure was performed in one of the two rooms according to our previous protocol
128 [38]. The dose of ICA was chosen on the basis of our previous experiments in rats showing that ICA had
129 a significant impact on behavior at 20 mg/kg [25].
130 The three groups exposed to CUMS underwent the sequence of stressors for 5 weeks, and were
131 administered with vehicle (saline 10 ml/kg), ICA (20 mg/kg), or Flx (10 mg/kg) by gavage at 11:00 a.m,
132 respectively, once daily for the 35 days of CUMS. After 5 weeks of CUMS exposure, rats were subjected
133 to different behavioral tests at least 16-18 h after the last dose. Time schedule and CUMS procedure of
134 experiments are illustrated in Figure 1.
135
136 **Behavioral Tests**
137 Before the experiment, the animals were allowed one week adaptation period. All experiments were
138 conducted between 8:00 am and 14:00 pm on the 35th day to minimize the impact of circadian rhythm
139 after the last treatment. In addition, rats were evaluated after 15 min of testing room habituation. Sucrose
140 Preference Test (SPT) was performed first, followed by Open field test (OFT), Elevated Plus-Maze
141 (EPM), and finally forced swimming test (FST) [39]. Double blindness was used for behavioral testing,
142 and all animals underwent behavioral tests. Experiments were performed and repeated 3 times.
143
144 **Sucrose Preference Test (SPT)**
145 The SPT is commonly used to quantify anhedonia was performed after five weeks and before surgery.
146 Briefly, all rats were first adapted to two bottles of 1% sucrose solution for 24 h. For the next 24 h, rats
147 were free to choose between a bottle of sterile water and a bottle of 1% sucrose solution. Prior to the test,

bioRxiv preprint doi: https://doi.org/10.1101/2023.03.09.531962; this version posted March 10, 2023. The copyright holder for this preprint (which was not certified by peer review) is the author/funder, who has granted bioRxiv a license to display the preprint in perpetuity. It is made available under aCC-BY 4.0 International license.

148 the rats were deprived of food and water for 23 h. Rats were then presented with two pre-weighted bottles
149 of sterile water and 1% sucrose solution. After 1 h, consumption of sucrose and water intake was
150 measured. Sucrose preference was calculated by the following formula: sucrose preference = sucrose
151 consumption/ [water consumption+ sucrose consumption] × 100% [40, 41].
152

153 **Elevated Plus-Maze (EPM)**

154 The procedure was performed as described previously [42]. Briefly, the EPM is 50cm high, which has
155 two enclosed (50 cm *10 cm *40 cm) and open (50 cm *10 cm) arms, the open central area is 10cm*10
156 cm area. Onset of the experiment, rats were placed in the central area, faced one of the enclosed arms.
157 The experiment was recorded on a video recording system in the next room for five minutes. The video
158 system records the frequency and time the rats entered the Open arms during the testing time. (RD1108-
159 EPM-R, Shanghai Mobile Datum Corporation, Shanghai, China).
160

161 **Open Field Test (OFT)**

162 The OFT was conducted as described by Yan et al [43]. The open field is a 100 × 100×40 cm cuboid box
163 with the black odorless plastic floor divided into 25 squares. The surrounding 16 squares were considered
164 as the peripheral zone, while the remaining 9 squares were regarded as central zone (regards as the social
165 area). The movements of rats in the peripheral zone were defined as protected behavior and the
166 movements in the central zone were defined as exploratory behavior. Rats were putted in the central zone
167 and their movements were recorded for 5 minutes with a video system. The number of entries in the
168 central zone, the total time expended in the central zone and defecation were scored.
169

170 **Forced Swim Test (FST)**

171 The FST described by Porsolt et al [44] was lightly alteration [40]. In brief, each rat was placed

bioRxiv preprint doi: https://doi.org/10.1101/2023.03.09.531962; this version posted March 10, 2023. The copyright holder for this preprint (which was not certified by peer review) is the author/funder, who has granted bioRxiv a license to display the preprint in perpetuity. It is made available under aCC-BY 4.0 International license.

172 individually in a cylindrical plexiglass container (diameter: 18 cm, height: 50 cm) with 7-8 liters of water
173 at 23±1 °C. The rats were put in the container for a 15 min training; 24 hours later, the rats were put in
174 the container again for another 5 mins test. The immobility time during the test was recorded by two
175 observers blinded to the experiment.

176

177 **Serum CORT assay**

178 After the FST procedure, blood samples were collected individually by intracardiac puncture between
179 11:00 am and 13:00 pm to avoid fluctuations in hormone levels. And separated in a refrigerated centrifuge
180 at 3,000 rpm for 15 min at 4 °C. Serum was stored at −80 °C till the assays. Tested the CORT
181 concentration with ELISA kit. The OD value at 405 nm was measured on an ELISA plate reader. CORT
182 concentration was quantitatively determined by comparing with the standard curve. Detection threshold
183 = 150 pg/mL, coefficient of variation limit =9.6%, and concentration expressed in pg/mL [45].

184

185 **Nissl Staining**

186 After the behavior testing, the rats were sacrificed immediately with anesthesia and perfused by trans-
187 cardiac with 4% para-formaldehyde in 0.1 M phosphate buffer. The brain tissues were dissected and
188 immersed the same concentration of formaldehyde. The brain tissues contained hippocampus were
189 embedded with paraffin and cut into 8 μm thick serial sections. The sections were stained with Cresyl
190 Violet and mages were taken at ×200 magnification with a microscope (Olympus AX-70) [39]. We
191 examined the morphology of neurons in the dorsal hippocampus of both hemispheres.

192

193 **In situ labeling of DNA fragmentation**

194 Apoptotic cells were detected by TUNNEL assay. 8 μm thickness coronal sections were putted in 1x
195 terminal deoxynucleotidyl transferase buffer (Invitrogen, Carlsbad, CA) for 30 min, then, they reacted

bioRxiv preprint doi: https://doi.org/10.1101/2023.03.09.531962; this version posted March 10, 2023. The copyright holder for this preprint (which was not certified by peer review) is the author/funder, who has granted bioRxiv a license to display the preprint in perpetuity. It is made available under aCC-BY 4.0 International license.

196 with terminal deoxynucleotidyl transferase enzyme (Invitrogen) and biotinylated 16-dUTP (Roche
197 Diagnostics, Indianapolis, IN) at 37 °C for 60 min. The slices were washed with 2x SSC (150 mol/liter
198 sodium chloride and 15 mol/liter sodium citrate, pH 7.4) for 15 min, and then washed with PBS for 15
199 mins two times again. Counterstaining nuclei with methyl green solution using avidin-biotin technique
200 [46].
201

202 **Mitochondrial Fractionation**

203 Fresh hippocampal tissue was weighed (100 mg) and washed with pre-cooled PBS and cut into fragments,
204 then the hippocampal debris were homogenized with a Dounce homogenizer on ice at 700 μL bovine
205 serum albumin (BSA)/Reagent A Solution. Mitochondria Isolation Reagent C (700 μL) was added to the
206 tube and centrifuged at 700 × *g* for 10 min at 4 °C to remove nuclei and unbroken cells. Transferred the
207 supernatant into a new tube and centrifuged at 11,000 × *g* for 15 min at 4 °C, the sediments we got were
208 just the mitochondria. And the supernatant was then transferred into another tube and centrifuged at
209 12,000 × g for 10 min at 4 °C to get the cytoplasmic without mitochondria [47]. Both the pellet
210 (mitochondria fraction) and the supernatant (cytoplasmic fraction) were stored for further testing.
211 Cytoplasmic and mitochondria fractions purity was confirmed by incubating specific antibodies against
212 β-tubulin (T9026, Sigma) and mHsp70 (MA3-028, Affinity Bioreagents) for each compartment,
213 respectively [48]. Representative blots demonstrating the purity of compartments are presented in Figure
214 S1. All samples exhibited proper separation, and no sample separation was unclear.
215

216 **Western blots**

217 Extracted the cytoplasm and mitochondria protein from the hippocampus, quantified the protein
218 concentrations with BCA (Beyotime, China). Loading buffer (0.1 MTris-HCl buffer (pH 6.8) containing
219 0.2 M DTT, 4% SDS, 20% glycerol and 0.1% bromophenol blue) was used to dissolve 40-60 μg equal

bioRxiv preprint doi: https://doi.org/10.1101/2023.03.09.531962; this version posted March 10, 2023. The copyright holder for this preprint (which was not certified by peer review) is the author/funder, who has granted bioRxiv a license to display the preprint in perpetuity. It is made available under aCC-BY 4.0 International license.

220 volume protein samples. The samples were separated on 10% SDS-PAGE and then electrically
221 transferred to PVDF membrane at 90 V. PVDF membranes were incubated with TBST (containing 5%
222 skimmed milk) for 1 h at 37 °C and with primary antibodies at 4 °C for 24 h. The primary antibodies
223 used were as follows: mouse anti-Bax, mouse anti-GR (1:1000), mouse anti-bcl-2, (1:400, SantaCruz
224 Biotechnology, USA), anti-β-actin, anti-Cox-IV, anti-caspase-3, cleaved caspase-3, anti-cytochrome c
225 (1:1000, Bioworld Technology, China). The blots were thoroughly washed with TBST and incubated at
226 37 °C with the secondary antibody in TBST containing 5% skimmed milk powder for 1 h. After that, the
227 signal was tested by enhanced chemiluminescence (ECL kit, Millipore, USA). Cox-IV was used as an
228 internal reference for proteins in mitochondria, while β-actin was used in cytoplasm. The membranes
229 were imaged and analyzed using the Quantity One Image Analysis Software (Syngene, U.K.) [49].
230
231 **Statistics analysis**
232 SPSS 20.0 software was used to analysis the data, and the data was appeared as mean ± SD. Compare
233 the mean using one-way analysis of variance (ANOVA). Several comparative tests were also conducted.
234 In addition, variance homogeneity test was used to test the data. The mean values of homogenous
235 variances were compared by ANOVA and analyzed the differences between the two groups using least
236 significant difference (LSD). If the data did not obey the normal distribution or the variance was uneven,
237 Welch's t-test was used, and the Games-Howell test was used for further pairwise comparison [50].
238 Differences were considered significant when P <0.05.
239
240 **Results**
241 The present study aimed to explore the potential neuronal apoptosis mechanism of hippocampus of
242 depression-like behaviors in CUMS-induced rats by investigating the function of ICA. Through a series
243 of *in vivo* experiments, it was found that ICA ameliorated neuronal apoptosis via inhibiting GR

bioRxiv preprint doi: https://doi.org/10.1101/2023.03.09.531962; this version posted March 10, 2023. The copyright holder for this preprint (which was not certified by peer review) is the author/funder, who has granted bioRxiv a license to display the preprint in perpetuity. It is made available under aCC-BY 4.0 International license.

244 mitochondrial translocation and expression of Bax, thereby preventing the release of cytochrome C into
245 the cytoplasm to activate caspase 3. Therefore, in the data, the function and mechanism of ICA were
246 studied, providing new insights into the pathogenesis of depression.
247

248 **ICA ameliorates CUMS-induced depression-like behaviors in rats**

249 First, the body weight was no significant difference among the four groups of rats at the beginning. From
250 1 to week 5, the body weight in the CUMS group was significantly lower than that of rats in control
251 group from week one to week 5. Specifically, upon the administration of CUMS+ICA and CUMS+Flx,
252 the body weight of the rats increased compared to those of the rats in the CUMS group at the end of the
253 experiment (Figure 2A). On the 35th day, there were significant differences in sucrose preference among
254 the four groups, with the lowest and highest sucrose preference percentages in the CUMS group and the
255 control group, respectively. Compared with the CUMS group, the CUMS+ICA and CUMS+Flx groups
256 showed significantly higher sucrose preference, suggesting that ICA may reduce anhedonia behavior of
257 rats (Figure 2B). EPM and the OFT test were first used to evaluate the locomotor behaviors and anxiety
258 of rats. For OFT test, the CUMS group showed the less time spent and entry frequency in the center zone,
259 while, ICA treatment significantly reversed this phenomenon, and Flx group showed a similar effect
260 (Figure 2C). As shown in Figure 2D, compared with the control group, all the stressed rats showed a
261 significant less frequently and lower time spent in the open arms, while ICA and Flx treatment could
262 increase the time spent and frequency in the open arms compared with CUMS group. As for the FST, the
263 immobility time and frequency of the rats in the CUMS group was significantly increased compared with
264 those of the rats in the control group, while the CUMS+ICA and CUMS+Flx groups reduced the
265 immobility time and frequency induced by CUMS group in rats (Figure 2E). Defecation in the open field
266 is always regarded as an index of the animal anxious state. But in our research, defecation among different
267 groups was only slightly different, and there was no significant difference (Fig.2F). Some studies [51,

bioRxiv preprint doi: https://doi.org/10.1101/2023.03.09.531962; this version posted March 10, 2023. The copyright holder for this preprint (which was not certified by peer review) is the author/funder, who has granted bioRxiv a license to display the preprint in perpetuity. It is made available under aCC-BY 4.0 International license.

268 52] confirmed that circulating CORT is associated with depression, so we measured the CORT levels in
269 serum of the rats to assess the depression-like state. As shown in Figure 2G, the circulating CORT of
270 CUMS increased significantly, while ICA and Flx could decrease the serum CORT levels.
271

272 **ICA decreases neuronal apoptosis in the hippocampal CA1 area of the CUMS rats**

273 Multiple studies suggest that depression induces neuronal apoptosis in the hippocampal CA1subfield
274 [39, 53]. Nischeria is considered a morphological index of the neural cell function [54], while TUNNEL
275 staining is usually used to detect apoptosis [46]. Based on the available evidence, hippocampal neuron
276 morphology changes were observed using Nissl staining. In our results, the normal cell morphology,
277 clear nucleus and purple blue staining of Nissl bodies can be seen in the normal neurons of control,
278 CUMS+ICA and CUMS+Flx groups (Figure 3A, C, D), while the TUNNEL positive cells of CUMS
279 group are shown with apoptotic bodies and pyknotic nuclei (Fig.3F). Taking together, samples from rats
280 chronically administered with ICA showed that neurons in the CA1 subfield of the hippocampi were
281 effectively protected compared to the CUMS exposed rats.
282

283 **ICA prevents mitochondrial translocation of apoptotic proteins**

284 During stress, high concentration GC in serum can induce apoptosis by GR mitochondrial translocation
285 [55]. In the present study, GR and apoptosis-related protein (Bax and Bcl-2) expression in mitochondria
286 and cytoplasmic was detected by western blot (Figure 4A and E). Results showed that GR expression
287 was increased in mitochondria of CUMS exposure group (Figure 4B), while was significantly reduced
288 in cytoplasm (Figure 4F). This effect was significantly subverted by ICA and Flx treatment, indicating
289 that ICA can prevent the translocation of GR from cytoplasm to mitochondria. Similarly, Bax was
290 markedly increased both in the mitochondria and cytoplasm in CUMS group, while ICA and Flx
291 decreased the level of Bax compared with CUMS group (Figure 4C and G). It is well known that the

bioRxiv preprint doi: https://doi.org/10.1101/2023.03.09.531962; this version posted March 10, 2023. The copyright holder for this preprint (which was not certified by peer review) is the author/funder, who has granted bioRxiv a license to display the preprint in perpetuity. It is made available under aCC-BY 4.0 International license.

292 ratio of Bax/Bcl-2 determines the death or survival fate of cell after apoptotic stimulus [56]. In addition,
293 Bcl-2 can regulate MOMP by combination with Bax [57]. In our study, the Bax/Bcl-2 ratio was also
294 analyzed. The data demonstrated that whether in mitochondria or cytoplasm, Bax/Bcl-2 ratio was
295 significantly increased under the stimulation of CUMS compared with the control group, indicating that
296 apoptosis was promoted, and the administration of ICA and Flx decreased the ratio, revealing that the
297 pro-apoptotic ability of CUMS was inhibited (Figure 4D and H).
298

299 **ICA inhibits caspase activation and cytochrome C release to the cytoplasm in hippocampus**

300 Caspase 3 is the main terminal processing protease and it plays a vital role in cell apoptosis [41]. The
301 release of cytochrome C into the cytoplasm can activate caspase-3, thereby inducing apoptosis [58]. In
302 our study, upon the administration of CUMS, caspase-3 (Figure 5B), cleaved caspase-3 (Figure 5C) and
303 cytochrome C (Figure 5D) expression was increased in the cytoplasm. While under the stimulation of
304 ICA and Flx, the expression of all three proteins decreased compared with the CUMS group. Indicating
305 that the level of cytochrome C extravasation into the cytoplasm is reduced, thereby inhibiting the
306 activation of caspase-3. The above results indicated that ICA can inhibit the MOMP induced by the Bax,
307 thereby preventing the release of cytochrome C into the cytoplasm to cause the activation of caspase-3,
308 and inhibiting the apoptosis of neuronal cells through the Bax/cytochrome C/caspase-3 axis.
309

310 **Discussion**

311 ICA is one of the most bio-active compounds purified from the Chinese herb *Epimedium*. Our previous
312 study verifies its broad-spectrum effects on antioxidant [59], anti-tumor [60, 61], anti-inflammation [29]
313 and anti-depression [62]. For example, Zeng et al. have proved that ICA can prevent depression and
314 dysfunctional hippocampal neurogenesis by regulating the certain proteins expression in the
315 cerebrospinal fluid [63]. Otherwise, Liu et al. revealed that ICA exerts antidepressant-like effects on

bioRxiv preprint doi: https://doi.org/10.1101/2023.03.09.531962; this version posted March 10, 2023. The copyright holder for this preprint (which was not certified by peer review) is the author/funder, who has granted bioRxiv a license to display the preprint in perpetuity. It is made available under aCC-BY 4.0 International license.

316 brain tissue by inhibiting of NF-κB signaling activation and enhancing antioxidant status and anti-
317 inflammatory effects by the NLRP3-inflammasome/caspase-1/IL-1β axis [26]. In this study, we analyzed
318 the effect of ICA using the known antidepressant drug Flx as a positive control, and the results
319 documented that five weeks' administration of ICA prevented the depressant-like behaviors of male rats
320 induced by CUMS and attenuated the hippocampal neuron apoptosis, which consistent with the effect of
321 Flx, and even some effects are better than Flx, such as suppressing the ratio of Bax/Bcl-2. Hence our
322 results support the idea that ICA exerts anti-depressant effects.
323 GR is a member of the steroid receptor superfamily [66], and the inactive form of GR is related to Hsp-
324 90 in the cytoplasm [67]. In the selection process of GR signal regulated thymocytes, mitochondria can
325 act as an important signal-integrator organelles [18]. Interestingly, GR signaling plays an important
326 regulatory role in hippocampal selection and apoptosis [68]. When GCs bind to their receptor, GR is
327 isolated from Hsp-90 and translocated to the nucleus, where it binds to the target genes and acts as a
328 transcription factor [69]. In physiological conditions, GCs are secreted by the adrenal cortex, regulate the
329 biosynthesis and metabolism of sugar, fat and protein [70], and it also play an important role in the anti-
330 inflammatory process [71]. Conversely, during pathological conditions, GCs combine with the GR,
331 inducing the expression of apoptosis proteins in the cells [72]. The fact that mitochondria directed GR
332 induces apoptosis suggests that the exclusive expression of GR in mitochondria is sufficient to trigger
333 apoptosis [55]. The decrease of mitochondrial GR level detected in males may help to mitigate the
334 adverse effects of LPS on mitochondrial signaling [73]. CORT is also secreted by the adrenal gland upon
335 stress exposure, and multiple studies proved the tight relationship between CORT and depression [74,
336 75]. Repeated CORT injections in animals result in HPA axis deregulation, cognitive, memory decline
337 and neuronal damage, and induce depression-like behavior [76, 77]. In addition to the well-understood
338 mechanism of CORT, it can also affect mitochondrial functions through binding with the GR within the
339 brain cells and brain tissues [78, 79]. There is evidence that compared with the healthy control group, the

bioRxiv preprint doi: https://doi.org/10.1101/2023.03.09.531962; this version posted March 10, 2023. The copyright holder for this preprint (which was not certified by peer review) is the author/funder, who has granted bioRxiv a license to display the preprint in perpetuity. It is made available under aCC-BY 4.0 International license.

340 GCs level of men who meet the criteria for MDD standard is significantly higher in men compared with
341 healthy controls, whereas no difference is observed in depressed women, and female rats have higher
342 baseline levels of CORT than males [80]. In addition, Brkic et al. revealed that alterations in
343 mitochondrial GR were more prominent in the PFC of males [48]. Therefore, in order to make the results
344 more significant and informative, we choose male rats to establish the animal model. In our study, during
345 exposure to CUMS, in spite of a marked increase in serum CORT, the level of cytoplasmic GR decreased
346 while mitochondrial GR increased. Thus, it seemed that chronic stress caused redistribution of GR by a
347 CORT independent mechanism.
348 Bax is the main pro-apoptotic protein of the Bcl-2 family which plays an important role in cell apoptosis
349 [81, 82]. Normally, Bax is located in the cytoplasm; it can aggregate into homologous dimers or combine
350 with Bcl-2 to form heterologous dimers [83, 84]. Bax plays an important role in the process of apoptosis
351 as Bax homodimers can bind to the mitochondrial outer membrane, resulting in an increase of MOMP
352 [85, 86]. After Bax formed pores on the mitochondrial outer membrane, cytochrome C is released into
353 the cytoplasm, which is involved in the formation of the apoptosome in conjunction with Apaf1 and
354 caspase-9 and activated caspase-3 [18] , after which caspase-3 degrades caspase-activated
355 deoxyribonuclease (CAD). CAD is then released and enters the nucleus to destroy DNA at the
356 nucleosome joint region [87-89]. However, Bcl-2 can regulate mitochondrial membrane permeability by
357 combination with Bax, and then control the release of cytochrome C [90]. Our results show that ICA can
358 reduce the expression of Bax and GR in mitochondria increased by CUMS. In line with this result, the
359 release of cytochrome C into the cytoplasm was inhibited by ICA, further preventing the activation of
360 caspase-3. In summary, our results confirmed that ICA related to its inhibition of neuronal apoptosis in
361 hippocampus through mitochondrial apoptotic pathway. However, some limitations of our study also
362 exist. For example, Luo et al. reported that GR translocation may be reduced under prolonged CUMS
363 stimulation [91]. We have not made a comparison for this, and further research is needed. In addition,

bioRxiv preprint doi: https://doi.org/10.1101/2023.03.09.531962; this version posted March 10, 2023. The copyright holder for this preprint (which was not certified by peer review) is the author/funder, who has granted bioRxiv a license to display the preprint in perpetuity. It is made available under aCC-BY 4.0 International license.

364 we did not detect differences in baseline corticosterone and GR in the sex group, which may indicate that
365 ICA did not produce any sex-specific lasting effect on the neuronal apoptosis. Therefore, in the following
366 work, we will establish a bisexual rat model to investigate whether this apoptotic mechanism is related
367 to sex.
368

369 **Conclusion**

370 Taken together, our research provide direct evidence that ICA played an antidepressant role in CUMS
371 rats by decreasing the GR mitochondrial translocation and reducing the neuronal apoptosis in the
372 hippocampus through a mitochondrial apoptotic pathway of Bax/cytoplasm C/caspase-3 axis. Our
373 current findings suggest that ICA may be an effective therapeutic treatment to prevent CUMS-induced
374 depression-like behaviors in rats.
375

376 **Disclosure statement**

377 **Ethics approval**

378 All experiments were conducted in line with the guidelines of Animal Care and Use Committee at
379 Affiliated Hospital of Nanjing University of Chinese Medicine(NO:HS-A-2021-0721). Every effort was
380 done to minimize the animals' suffering.

381 **Availability of data and materials**

382 The data used to support the findings of this study are available from the corresponding author upon
383 request.

384 **Conflict of interest**

385 The authors declare that they have no competing interests.

386 **Acknowledgements**

387 Not applicable.

388 **Funding**

bioRxiv preprint doi: https://doi.org/10.1101/2023.03.09.531962; this version posted March 10, 2023. The copyright holder for this preprint (which was not certified by peer review) is the author/funder, who has granted bioRxiv a license to display the preprint in perpetuity. It is made available under aCC-BY 4.0 International license.

389 This study was funded by grants from the National Natural Science Foundation of China (No: 81102562,
390 81904029), Natural Science Foundation of Jiangsu Science and Technology Department (No:
391 BK20201504), Intra-hospital Foundation of Jiangsu Provincial Hospital of Chinese Medicine (No:
392 Y20030, Y19064), Colleges and Universities in Jiangsu Province Natural Science Research (Grant
393 number 19KJB360010) and National Natural Science Foundation of Nanjing University of Chinese
394 Medicine (XZR2020004).

395

396

397 **References**

398 [1] Kendler KS, Sheth K, Gardner CO et al. Childhood parental loss and risk for first-onset of major
399 depression and alcohol dependence: the time-decay of risk and sex differences. Psychol Med.
400 2002;32(7):1187-1194.
401 [2] Collins PY, Patel V, Joestl SS et al. Grand challenges in global mental health. Nature.475(7354):27-
402 30.
403 [3] Andersen J, Stuhr-Hansen N, Zachariassen L et al. Molecular determinants for selective recognition
404 of antidepressants in the human serotonin and norepinephrine transporters. Proc Natl Acad Sci U S
405 A.108(29):12137-12142.
406 [4] Kemp AH, Brunoni AR, Santos IS et al. Effects of depression, anxiety, comorbidity, and
407 antidepressants on resting-state heart rate and its variability: an ELSA-Brasil cohort baseline study.
408 Am J Psychiatry.171(12):1328-1334.
409 [5] Patten SB, Williams JVA, Lavorato DH et al. Why is major depression prevalence not changing? J
410 Affect Disord. 2016;190:93-97.
411 [6] Huang YJ, Lane HY, Lin CH. New Treatment Strategies of Depression: Based on Mechanisms
412 Related to Neuroplasticity. Neural Plast. 2017;2017:4605971.

bioRxiv preprint doi: https://doi.org/10.1101/2023.03.09.531962; this version posted March 10, 2023. The copyright holder for this preprint (which was not certified by peer review) is the author/funder, who has granted bioRxiv a license to display the preprint in perpetuity. It is made available under aCC-BY 4.0 International license.

413 [7] Li S, Yang L, Zhang Y et al. Taurine Ameliorates Arsenic-Induced Apoptosis in the Hippocampus
414 of Mice Through Intrinsic Pathway. Adv Exp Med Biol. 2017;975 Pt 1:183-192.
415 [8] Wingenfeld K, Wolf OT. Stress, memory, and the hippocampus. Front Neurol Neurosci.34:109-
416 120.
417 [9] D'Sa C, Duman RS. Antidepressants and neuroplasticity. Bipolar Disord. 2002;4(3):183-194.
418 [10] Nestler EJ, Barrot M, DiLeone RJ et al. Neurobiology of depression. Neuron. 2002;34(1):13-25.
419 [11] McEwen BS, Gould EA, Sakai RR. The vulnerability of the hippocampus to protective and
420 destructive effects of glucocorticoids in relation to stress. Br J Psychiatry Suppl. 1992(15):18-23.
421 [12] Ding WX, Yin XM. Mitophagy: mechanisms, pathophysiological roles, and analysis. Biol Chem.
422 2012;393(7):547-564.
423 [13] Iwamoto K, Bundo M, Kato T. Altered expression of mitochondria-related genes in postmortem
424 brains of patients with bipolar disorder or schizophrenia, as revealed by large-scale DNA microarray
425 analysis. Hum Mol Genet. 2005;14(2):241-253.
426 [14] Gong Y, Chai Y, Ding JH et al. Chronic mild stress damages mitochondrial ultrastructure and
427 function in mouse brain. Neurosci Lett. 2011;488(1):76-80.
428 [15] De R, Mazumder S, Sarkar S et al. Acute mental stress induces mitochondrial bioenergetic crisis
429 and hyper-fission along with aberrant mitophagy in the gut mucosa in rodent model of stress-related
430 mucosal disease. Free Radic Biol Med. 2017;113:424-438.
431 [16] Manoli I, Alesci S, Blackman MR et al. Mitochondria as key components of the stress response.
432 Trends Endocrinol Metab. 2007;18(5):190-198.
433 [17] Lapp HE, Bartlett AA, Hunter RG. Stress and glucocorticoid receptor regulation of mitochondrial
434 gene expression. J Mol Endocrinol. 2019;62(2):R121-R128.
435 [18] Prenek L, Boldizsar F, Kugyelka R et al. The regulation of the mitochondrial apoptotic pathway by
436 glucocorticoid receptor in collaboration with Bcl-2 family proteins in developing T cells. Apoptosis.

bioRxiv preprint doi: https://doi.org/10.1101/2023.03.09.531962; this version posted March 10, 2023. The copyright holder for this preprint (which was not certified by peer review) is the author/funder, who has granted bioRxiv a license to display the preprint in perpetuity. It is made available under aCC-BY 4.0 International license.

437 2017;22(2):239-253.

438 [19] Yuan JY, Tong ZY, Dong YC et al. Research progress on icariin, a traditional Chinese medicine
439 extract, in the treatment of asthma. Allergol Immunopathol (Madr). 2022;50(1):9-16.

440 [20] Zhang Q, Xie L, Jiang L et al. Icariin attenuates renal fibrosis in vivo and in vitro by inhibiting the
441 Notch2/Hes-1 pathway. Growth Factors. 2022:1-11.

442 [21] Zhang Y, Wu X, Zhu K et al. Icariin attenuates perfluorooctane sulfonate-induced testicular toxicity
443 by alleviating Sertoli cell injury and downregulating the p38MAPK/MMP9 pathway. Food Funct.
444 2022;13(6):3674-3689.

445 [22] Tang W, Zhang H, Liu D et al. Icariin accelerates cartilage defect repair by promoting chondrogenic
446 differentiation of BMSCs under conditions of oxygen-glucose deprivation. J Cell Mol Med.
447 2022;26(1):202-215.

448 [23] Tang M, Chen M, Li Q. Paeoniflorin ameliorates chronic stress-induced depression-like behavior
449 in mice model by affecting ERK1/2 pathway. Bioengineered. 2021;12(2):11329-11341.

450 [24] Zhang Y, Luo Y, Hou X et al. Xiaoyao powder alleviates the hippocampal neuron damage in chronic
451 unpredictable mild stress-induced depression model rats in hippocampus via connexin
452 43Cx43/glucocorticoid receptor/brain-derived neurotrophic factor signaling pathway.
453 Bioengineered. 2022;13(1):383-394.

454 [25] Liu L, Zhao Z, Lu L et al. Icariin and icaritin ameliorated hippocampus neuroinflammation via
455 inhibiting HMGB1-related pro-inflammatory signals in lipopolysaccharide-induced inflammation
456 model in C57BL/6J mice. Int Immunopharmacol. 2019;68:95-105.

457 [26] Liu B, Xu C, Wu X et al. Icariin exerts an antidepressant effect in an unpredictable chronic mild
458 stress model of depression in rats and is associated with the regulation of hippocampal
459 neuroinflammation. Neuroscience. 2015;294:193-205.

460 [27] Zheng XX, Li YC, Yang KL et al. Icariin reduces Glu-induced excitatory neurotoxicity via

bioRxiv preprint doi: https://doi.org/10.1101/2023.03.09.531962; this version posted March 10, 2023. The copyright holder for this preprint (which was not certified by peer review) is the author/funder, who has granted bioRxiv a license to display the preprint in perpetuity. It is made available under aCC-BY 4.0 International license.

461 antioxidative and antiapoptotic pathways in SH-SY5Y cells. Phytother Res. 2021;35(6):3377-3389.
462 [28] Nian H, Ma MH, Nian SS et al. Antiosteoporotic activity of icariin in ovariectomized rats.
463 Phytomedicine. 2009;16(4):320-326.
464 [29] Li B, Duan X, Xu C et al. Icariin attenuates glucocorticoid insensitivity mediated by repeated
465 psychosocial stress on an ovalbumin-induced murine model of asthma. Int
466 Immunopharmacol.19(2):381-390.
467 [30] Li L, Sun J, Xu C et al. Icariin ameliorates cigarette smoke induced inflammatory responses via
468 suppression of NF-kappaB and modulation of GR in vivo and in vitro. PLoS One.9(8):e102345.
469 [31] Wu X, Wu J, Xia S et al. Icaritin opposes the development of social aversion after defeat stress via
470 increases of GR mRNA and BDNF mRNA in mice. Behav Brain Res.256:602-608.
471 [32] Liu B, Zhang H, Xu C et al. Neuroprotective effects of icariin on corticosterone-induced apoptosis
472 in primary cultured rat hippocampal neurons. Brain Res.1375:59-67.
473 [33] Li Z, Wang F, Zhang S. Knockdown of lncRNA MNX1-AS1 suppresses cell proliferation,
474 migration, and invasion in prostate cancer. FEBS Open Bio. 2019;9(5):851-858.
475 [34] Berton O, McClung CA, Dileone RJ et al. Essential role of BDNF in the mesolimbic dopamine
476 pathway in social defeat stress. Science. 2006;311(5762):864-868.
477 [35] Tian DD, Wang M, Liu A et al. Antidepressant Effect of Paeoniflorin Is Through Inhibiting
478 Pyroptosis CASP-11/GSDMD Pathway. Mol Neurobiol. 2021;58(2):761-776.
479 [36] Wei K, Xu Y, Zhao Z et al. Icariin alters the expression of glucocorticoid receptor, FKBP5 and
480 SGK1 in rat brains following exposure to chronic mild stress. Int J Mol Med. 2016;38(1):337-344.
481 [37] Zhang W, Qu W, Wang H et al. Antidepressants fluoxetine and amitriptyline induce alterations in
482 intestinal microbiota and gut microbiome function in rats exposed to chronic unpredictable mild
483 stress. Transl Psychiatry. 2021;11(1):131.
484 [38] Yang P, Gao Z, Zhang H et al. Changes in proinflammatory cytokines and white matter in

bioRxiv preprint doi: https://doi.org/10.1101/2023.03.09.531962; this version posted March 10, 2023. The copyright holder for this preprint (which was not certified by peer review) is the author/funder, who has granted bioRxiv a license to display the preprint in perpetuity. It is made available under aCC-BY 4.0 International license.

485 chronically stressed rats. Neuropsychiatr Dis Treat.11:597-607.

486 [39] Dang R, Wang M, Li X et al. Edaravone ameliorates depressive and anxiety-like behaviors via
487 Sirt1/Nrf2/HO-1/Gpx4 pathway. J Neuroinflammation. 2022;19(1):41.

488 [40] Wang AR, Mi LF, Zhang ZL et al. Saikosaponin A improved depression-like behavior and inhibited
489 hippocampal neuronal apoptosis after cerebral ischemia through p-CREB/BDNF pathway. Behav
490 Brain Res. 2021;403:113138.

491 [41] Shen J, Zhang P, Li Y et al. Neuroprotective effects of microRNA-211-5p on chronic stress-induced
492 neuronal apoptosis and depression-like behaviours. J Cell Mol Med. 2021;25(14):7028-7038.

493 [42] Pellow S, Chopin P, File SE et al. Validation of Open - Closed Arm Entries in an Elevated Plus-
494 Maze as a Measure of Anxiety in the Rat. Journal of Neuroscience Methods. 1985;14(3):149-167.

495 [43] Yan L, Xu X, He Z et al. Antidepressant-Like Effects and Cognitive Enhancement of
496 Coadministration of Chaihu Shugan San and Fluoxetine: Dependent on the BDNF-ERK-CREB
497 Signaling Pathway in the Hippocampus and Frontal Cortex. Biomed Res Int. 2020;2020:2794263.

498 [44] Porsolt RD, Lepichon M, Jalfre M. Depression - New Animal-Model Sensitive to Antidepressant
499 Treatments. Nature. 1977;266(5604):730-732.

500 [45] Kinlein SA, Phillips DJ, Keller CR et al. Role of corticosterone in altered neurobehavioral responses
501 to acute stress in a model of compromised hypothalamic-pituitary-adrenal axis function.
502 Psychoneuroendocrinology. 2019;102:248-255.

503 [46] Zamani M, Hassanshahi J, Soleimani M et al. Neuroprotective effect of olive oil in the hippocampus
504 CA1 neurons following ischemia: Reperfusion in mice. J Neurosci Rural Pract. 2013;4(2):164-170.

505 [47] Shu X, Sun Y, Sun X et al. The effect of fluoxetine on astrocyte autophagy flux and injured
506 mitochondria clearance in a mouse model of depression. Cell Death Dis. 2019;10(8):577.

507 [48] Brkic Z, Milosavljevic M, Glavonic E et al. Mitochondrial signaling in inflammation-induced
508 depressive behavior in female and male rats: The role of glucocorticoid receptor. Brain Res Bull.

bioRxiv preprint doi: https://doi.org/10.1101/2023.03.09.531962; this version posted March 10, 2023. The copyright holder for this preprint (which was not certified by peer review) is the author/funder, who has granted bioRxiv a license to display the preprint in perpetuity. It is made available under aCC-BY 4.0 International license.

509 2019;150:317-327.

510 [49] Bian H, Yan F, Li W et al. Tert-butylhydroquinone prevents neuroinflammation and relieves
511 depression via regulation of NLRP3 signaling in mice. Int Immunopharmacol. 2022;107:108723.

512 [50] Zhu X, Jing L, Chen C et al. Danzhi Xiaoyao San ameliorates depressive-like behavior by shifting
513 toward serotonin via the downregulation of hippocampal indoleamine 2,3-dioxygenase. J
514 Ethnopharmacol. 2015;160:86-93.

515 [51] Dubey VK, Ansari F, Vohora D et al. Possible involvement of corticosterone and serotonin in
516 antidepressant and antianxiety effects of chromium picolinate in chronic unpredictable mild stress
517 induced depression and anxiety in rats. J Trace Elem Med Biol.29:222-226.

518 [52] Wang ZJ, Yu B, Zhang XQ et al. Correlations between depression behaviors and sleep parameters
519 after repeated corticosterone injections in rats. Acta Pharmacol Sin.35(7):879-888.

520 [53] Ping F, Shang J, Zhou J et al. 5-HT(1A) receptor and apoptosis contribute to interferon-alpha-
521 induced "depressive-like" behavior in mice. Neurosci Lett.514(2):173-178.

522 [54] Wang J, Yue B, Zhang X et al. Effect of exercise on microglial activation and transcriptome of
523 hippocampus in fluorosis mice. Sci Total Environ. 2021;760:143376.

524 [55] Sionov RV, Cohen O, Kfir S et al. Role of mitochondrial glucocorticoid receptor in glucocorticoid-
525 induced apoptosis. J Exp Med. 2006;203(1):189-201.

526 [56] Mahdavi S, Khodarahmi P, Roodbari NH. Effects of cadmium on Bcl-2/ Bax expression ratio in rat
527 cortex brain and hippocampus. Hum Exp Toxicol. 2018;37(3):321-328.

528 [57] Gaudette BT, Dwivedi B, Chitta KS et al. Low expression of pro-apoptotic Bcl-2 family proteins
529 sets the apoptotic threshold in Waldenstrom macroglobulinemia. Oncogene. 2016;35(4):479-490.

530 [58] Brentnall M, Rodriguez-Menocal L, De Guevara RL et al. Caspase-9, caspase-3 and caspase-7 have
531 distinct roles during intrinsic apoptosis. BMC Cell Biol. 2013;14:32.

532 [59] Luo Y, Nie J, Gong QH et al. Protective effects of icariin against learning and memory deficits

bioRxiv preprint doi: https://doi.org/10.1101/2023.03.09.531962; this version posted March 10, 2023. The copyright holder for this preprint (which was not certified by peer review) is the author/funder, who has granted bioRxiv a license to display the preprint in perpetuity. It is made available under aCC-BY 4.0 International license.

533 induced by aluminium in rats. Clin Exp Pharmacol Physiol. 2007;34(8):792-795.

534 [60] Wang Q, Hao J, Pu J et al. Icariin induces apoptosis in mouse MLTC-10 Leydig tumor cells through
535 activation of the mitochondrial pathway and down-regulation of the expression of piwil4. Int J
536 Oncol.39(4):973-980.

537 [61] Zhou J, Wu J, Chen X et al. Icariin and its derivative, ICT, exert anti-inflammatory, anti-tumor
538 effects, and modulate myeloid derived suppressive cells (MDSCs) functions. Int
539 Immunopharmacol.11(7):890-898.

540 [62] Wu J, Du J, Xu C et al. Icariin attenuates social defeat-induced down-regulation of glucocorticoid
541 receptor in mice. Pharmacol Biochem Behav.98(2):273-278.

542 [63] Zeng NX, Li HZ, Wang HZ et al. Exploration of the mechanism by which icariin modulates
543 hippocampal neurogenesis in a rat model of depression. Neural Regen Res. 2022;17(3):632-642.

544 [64] Willner P. Chronic mild stress (CMS) revisited: consistency and behavioural-neurobiological
545 concordance in the effects of CMS. Neuropsychobiology. 2005;52(2):90-110.

546 [65] Czeh B, Fuchs E, Wiborg O et al. Animal models of major depression and their clinical implications.
547 Prog Neuropsychopharmacol Biol Psychiatry.

548 [66] Evans RM. The steroid and thyroid hormone receptor superfamily. Science. 1988;240(4854):889-
549 895.

550 [67] Smith DF, Toft DO. Steroid receptors and their associated proteins. Mol Endocrinol. 1993;7(1):4-
551 11.

552 [68] Lengel D, Romm ZL, Bostwick AL et al. Glucocorticoid Receptor Overexpression in the Dorsal
553 Hippocampus Attenuates Spatial Learning and Synaptic Plasticity Deficits Following Pediatric
554 Traumatic Brain Injury. J Neurotrauma. 2022.

555 [69] Berg JM. DNA binding specificity of steroid receptors. Cell. 1989;57(7):1065-1068.

556 [70] Cavigelli SA, Caruso MJ. Sex, social status and physiological stress in primates: the importance of

bioRxiv preprint doi: https://doi.org/10.1101/2023.03.09.531962; this version posted March 10, 2023. The copyright holder for this preprint (which was not certified by peer review) is the author/funder, who has granted bioRxiv a license to display the preprint in perpetuity. It is made available under aCC-BY 4.0 International license.

557 social and glucocorticoid dynamics. Philos Trans R Soc Lond B Biol Sci.370(1669).

558 [71] Vago JP, Tavares LP, Garcia CC et al. The role and effects of glucocorticoid-induced leucine zipper
559 in the context of inflammation resolution. J Immunol.194(10):4940-4950.

560 [72] Matthews LC, Berry AA, Morgan DJ et al. Glucocorticoid receptor regulates accurate chromosome
561 segregation and is associated with malignancy. Proc Natl Acad Sci U S A.112(17):5479-5484.

562 [73] Sionov RV, Kfir S, Zafrir E et al. Glucocorticoid-induced apoptosis revisited: a novel role for
563 glucocorticoid receptor translocation to the mitochondria. Cell Cycle. 2006;5(10):1017-1026.

564 [74] Moloney RD, Dinan TG, Cryan JF. Strain-dependent variations in visceral sensitivity: relationship
565 to stress, anxiety and spinal glutamate transporter expression. Genes Brain Behav.14(4):319-329.

566 [75] Vasconcelos AS, Oliveira IC, Vidal LT et al. Subchronic administration of riparin III induces
567 antidepressive-like effects and increases BDNF levels in the mouse hippocampus. Fundam Clin
568 Pharmacol.

569 [76] Badr AM, Attia HA, Al-Rasheed N. Oleuropein Reverses Repeated Corticosterone-Induced
570 Depressive-Like Behavior in mice: Evidence of Modulating Effect on Biogenic Amines. Sci Rep.
571 2020;10(1):3336.

572 [77] Chai Y, Cai Y, Fu Y et al. Salidroside Ameliorates Depression by Suppressing NLRP3-Mediated
573 Pyroptosis via P2X7/NF-kappaB/NLRP3 Signaling Pathway. Front Pharmacol. 2022;13:812362.

574 [78] Koufali MM, Moutsatsou P, Sekeris CE et al. The dynamic localization of the glucocorticoid
575 receptor in rat C6 glioma cell mitochondria. Mol Cell Endocrinol. 2003;209(1-2):51-60.

576 [79] Moutsatsou P, Psarra AM, Tsiapara A et al. Localization of the glucocorticoid receptor in rat brain
577 mitochondria. Arch Biochem Biophys. 2001;386(1):69-78.

578 [80] Bangasser DA, Wicks B. Sex-specific mechanisms for responding to stress. J Neurosci Res.
579 2017;95(1-2):75-82.

580 [81] Chipuk JE, Moldoveanu T, Llambi F et al. The BCL-2 family reunion. Mol Cell.37(3):299-310.

bioRxiv preprint doi: https://doi.org/10.1101/2023.03.09.531962; this version posted March 10, 2023. The copyright holder for this preprint (which was not certified by peer review) is the author/funder, who has granted bioRxiv a license to display the preprint in perpetuity. It is made available under aCC-BY 4.0 International license.

581 [82] Ola MS, Nawaz M, Ahsan H. Role of Bcl-2 family proteins and caspases in the regulation of
582 apoptosis. Mol Cell Biochem.351(1-2):41-58.
583 [83] Tait SW, Green DR. Mitochondria and cell death: outer membrane permeabilization and beyond.
584 Nat Rev Mol Cell Biol.11(9):621-632.
585 [84] Martinou JC, Youle RJ. Mitochondria in apoptosis: Bcl-2 family members and mitochondrial
586 dynamics. Dev Cell.21(1):92-101.
587 [85] Edlich F, Banerjee S, Suzuki M et al. Bcl-x(L) retrotranslocates Bax from the mitochondria into the
588 cytosol. Cell. 2011;145(1):104-116.
589 [86] Talaber G, Boldizsar F, Bartis D et al. Mitochondrial translocation of the glucocorticoid receptor in
590 double-positive thymocytes correlates with their sensitivity to glucocorticoid-induced apoptosis. Int
591 Immunol. 2009;21(11):1269-1276.
592 [87] Fellows E, Gil-Parrado S, Jenne DE et al. Natural killer cell-derived human granzyme H induces an
593 alternative, caspase-independent cell-death program. Blood. 2007;110(2):544-552.
594 [88] Zou H, Henzel WJ, Liu X et al. Apaf-1, a human protein homologous to C. elegans CED-4,
595 participates in cytochrome c-dependent activation of caspase-3. Cell. 1997;90(3):405-413.
596 [89] Porter AG, Janicke RU. Emerging roles of caspase-3 in apoptosis. Cell Death Differ. 1999;6(2):99-
597 104.
598 [90] Gaudette BT, Dwivedi B, Chitta KS et al. Low expression of pro-apoptotic Bcl-2 family proteins
599 sets the apoptotic threshold in Waldenstrom macroglobulinemia. Oncogene.
600 [91] Luo S, Hou Y, Zhang Y et al. Bag-1 mediates glucocorticoid receptor trafficking to mitochondria
601 after corticosterone stimulation: Potential role in regulating affective resilience. J Neurochem.
602 2021;158(2):358-372.
603

604 **Figure Legends**

bioRxiv preprint doi: https://doi.org/10.1101/2023.03.09.531962; this version posted March 10, 2023. The copyright holder for this preprint (which was not certified by peer review) is the author/funder, who has granted bioRxiv a license to display the preprint in perpetuity. It is made available under aCC-BY 4.0 International license.

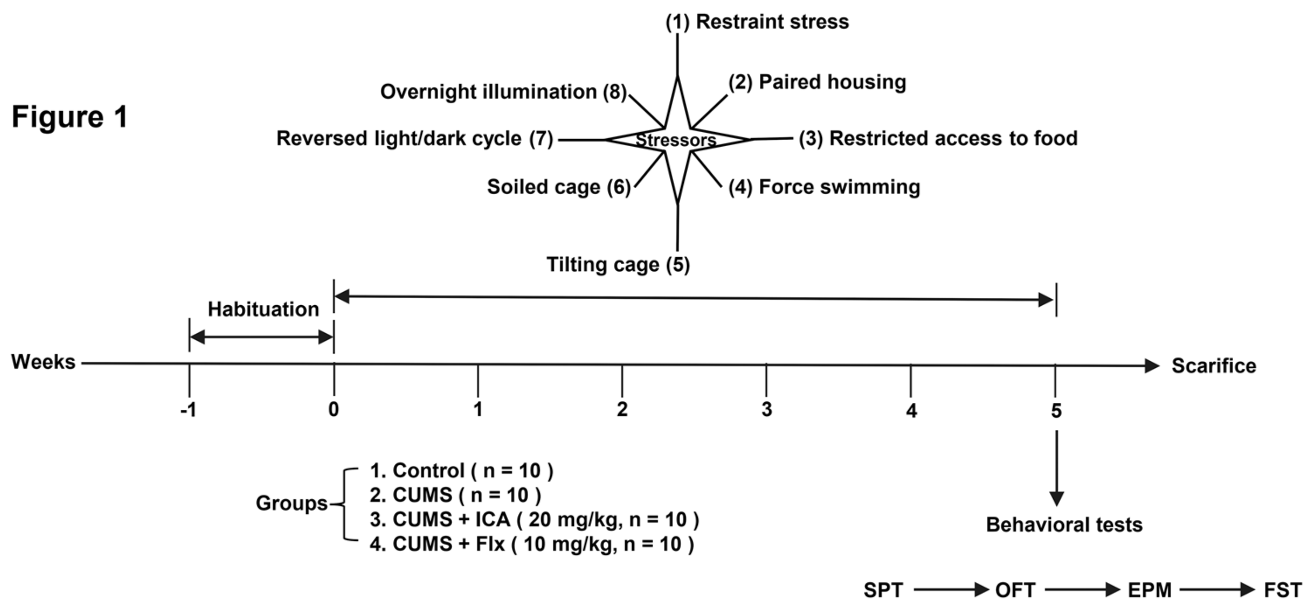

605

606 **Fig.1** Timeline of the experiment. Before the experiment, the animals were allowed a 7-days adaptation
607 period. Except for the control group, the rats in the other groups were subjected to CUMS for 5 weeks
608 and treated with different drugs. CUMS procedure was performed in random order. The body weights
609 were monitored weekly. SPT, OFT, EPM and FST were performed in order at day 35. Then, the rats
610 were sacrificed for further detection.

bioRxiv preprint doi: https://doi.org/10.1101/2023.03.09.531962; this version posted March 10, 2023. The copyright holder for this preprint (which was not certified by peer review) is the author/funder, who has granted bioRxiv a license to display the preprint in perpetuity. It is made available under aCC-BY 4.0 International license.

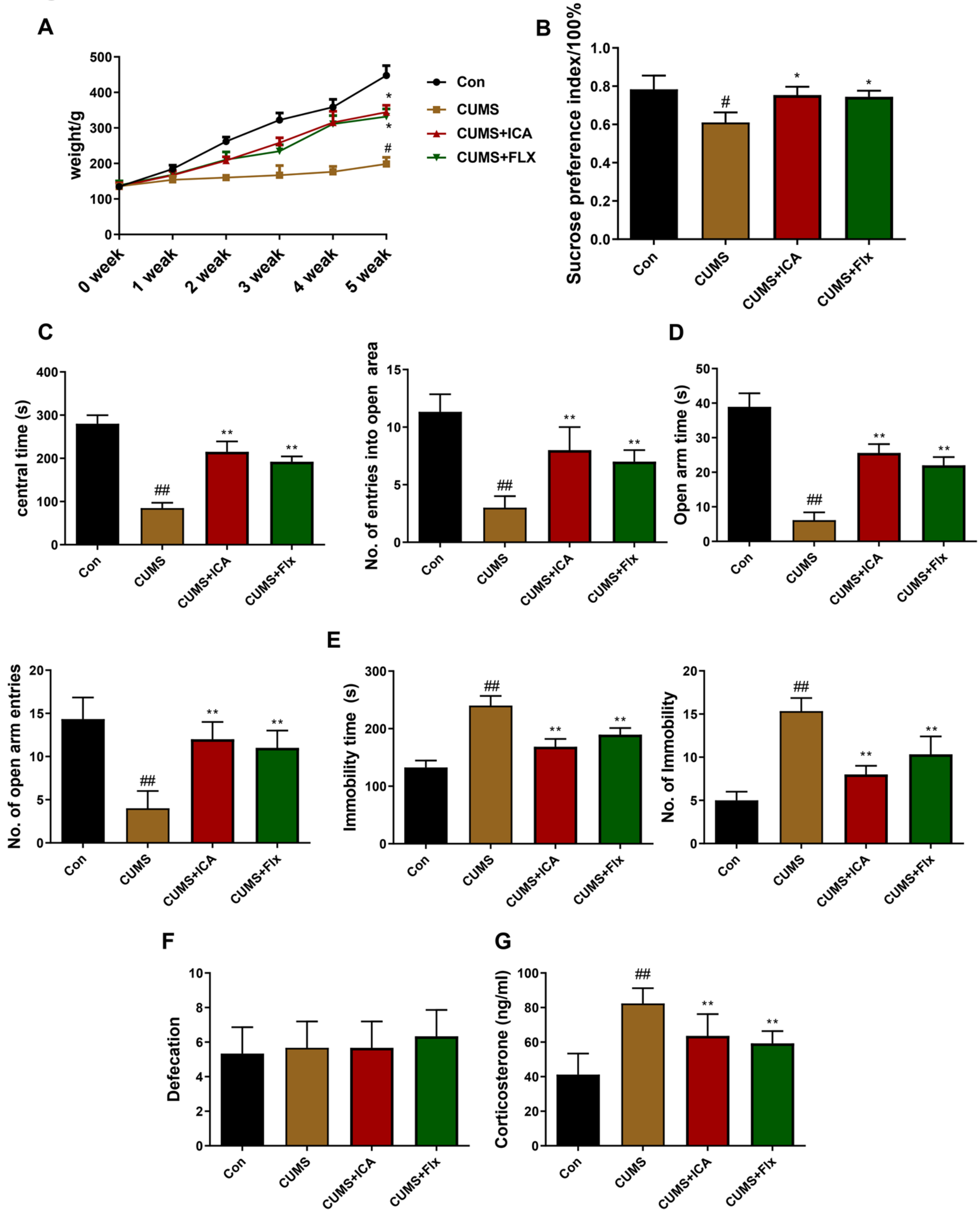

611

612 **Fig. 2 Effects of ICA**

613 **on the body weight and behavior of rats subjected to different groups.** 40 rats were divided into 4

614 groups (10 rats/group) and treated with Control, CUMS-vehicle (saline 10 ml/kg), CUMS-icariin (20

bioRxiv preprint doi: https://doi.org/10.1101/2023.03.09.531962; this version posted March 10, 2023. The copyright holder for this preprint (which was not certified by peer review) is the author/funder, who has granted bioRxiv a license to display the preprint in perpetuity. It is made available under aCC-BY 4.0 International license.

615 mg/kg) and CUMS-Flx (positive control, 10 mg/kg) separately for 5 weeks. (A) Changes in body weight
616 from week 0 to week 5. $^{\#}P < 0.05$ vs. Control group, $^{*}P < 0.05$ vs. CUMS group. df=10. (B) Sucrose
617 preference among study groups at day 35. $^{\#}P < 0.05$ vs. Control group, $^{*}P < 0.05$ vs. CUMS group. df=11.
618 (C) FST immobile time and frequency. $^{\#\#}P < 0.05$ vs. Control group, $^{**}P < 0.05$ vs. CUMS group. df=11.
619 (D) Time and frequency of enter the open arm. $^{\#\#}P < 0.05$ vs. Control group, $^{**}P < 0.05$ vs. CUMS group.
620 df=11. (E) OFT center time and frequency were measured. $^{\#\#}P < 0.05$ vs. Control group, $^{**}P < 0.05$ vs.
621 CUMS group. df=11. (F) The defecation of rats in open field. (G) The CORT in the serum of rats with
622 different groups. $^{\#\#}P < 0.01$ vs. Control group; **P < 0.01 vs. CUMS group. df=11. Data were presented
623 as the mean + SD (n = 10 per group).

bioRxiv preprint doi: https://doi.org/10.1101/2023.03.09.531962; this version posted March 10, 2023. The copyright holder for this preprint (which was not certified by peer review) is the author/funder, who has granted bioRxiv a license to display the preprint in perpetuity. It is made available under aCC-BY 4.0 International license.

Figure 3

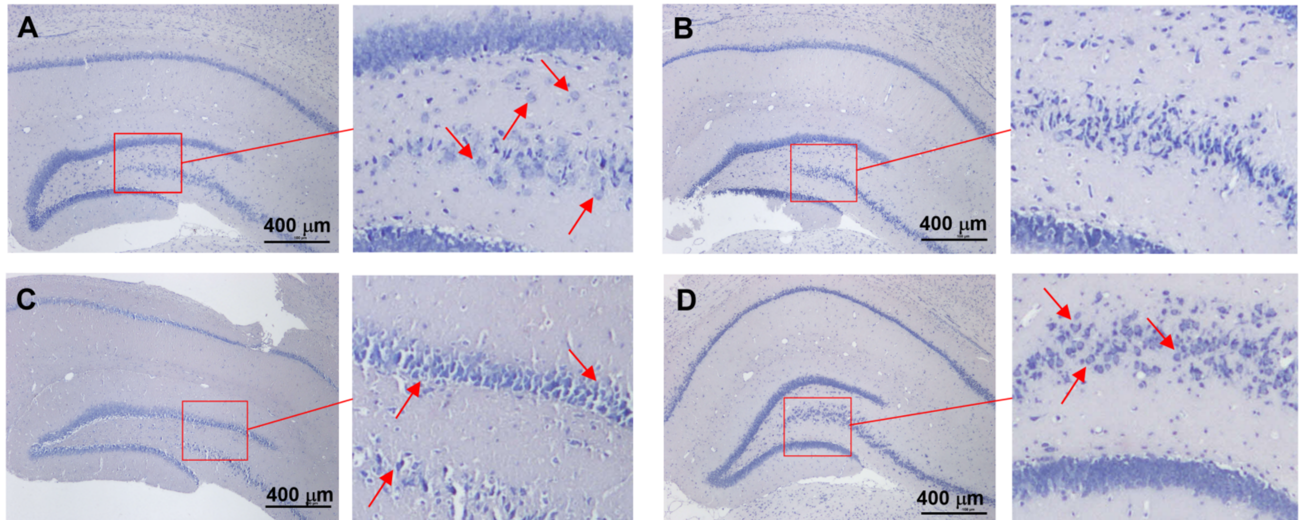

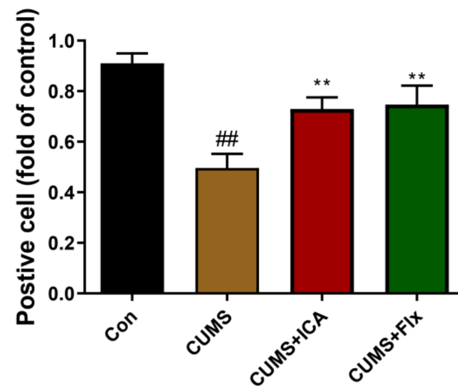

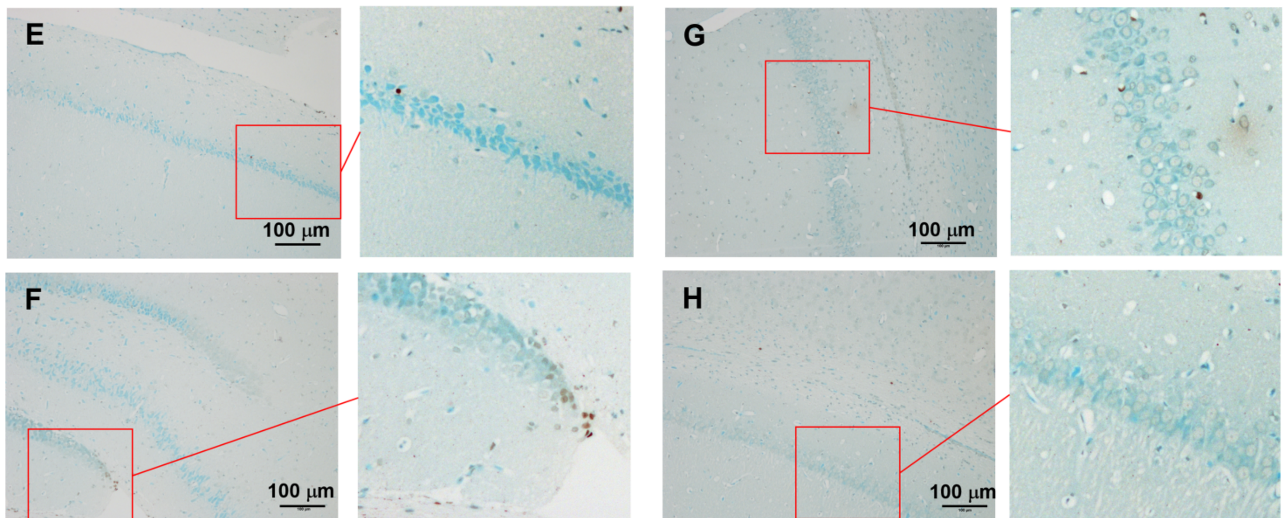

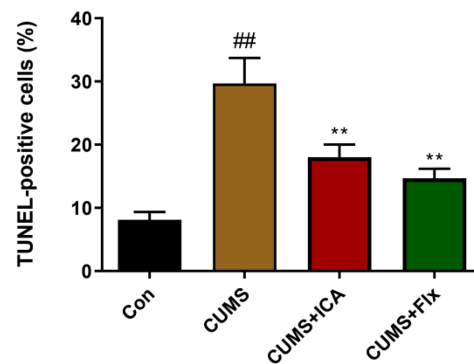

624

bioRxiv preprint doi: https://doi.org/10.1101/2023.03.09.531962; this version posted March 10, 2023. The copyright holder for this preprint (which was not certified by peer review) is the author/funder, who has granted bioRxiv a license to display the preprint in perpetuity. It is made available under aCC-BY 4.0 International license.

625 **Fig.3 Photomicrographs of hippocampal pathological sections.** (A)-(D) Nissl staining of CA1 region
626 in hippocampus. (E)-(F) TUNNEL staining of CA1 region in hippocampus. (A), (E) are Con group; (B),
627 (F) are CUMS group; (C), (G) are ICA group; (D), (H) are Flx group. The red arrows indicate the Nissl
628 bodies and apoptotic bodies. Data were presented as the mean + SD (n = 10 per group). $^{##}p < 0.01$ vs.
629 Control group; $^{**}p < 0.01$ vs. CUMS group, df=11.

bioRxiv preprint doi: https://doi.org/10.1101/2023.03.09.531962; this version posted March 10, 2023. The copyright holder for this preprint (which was not certified by peer review) is the author/funder, who has granted bioRxiv a license to display the preprint in perpetuity. It is made available under aCC-BY 4.0 International license.

Figure 4

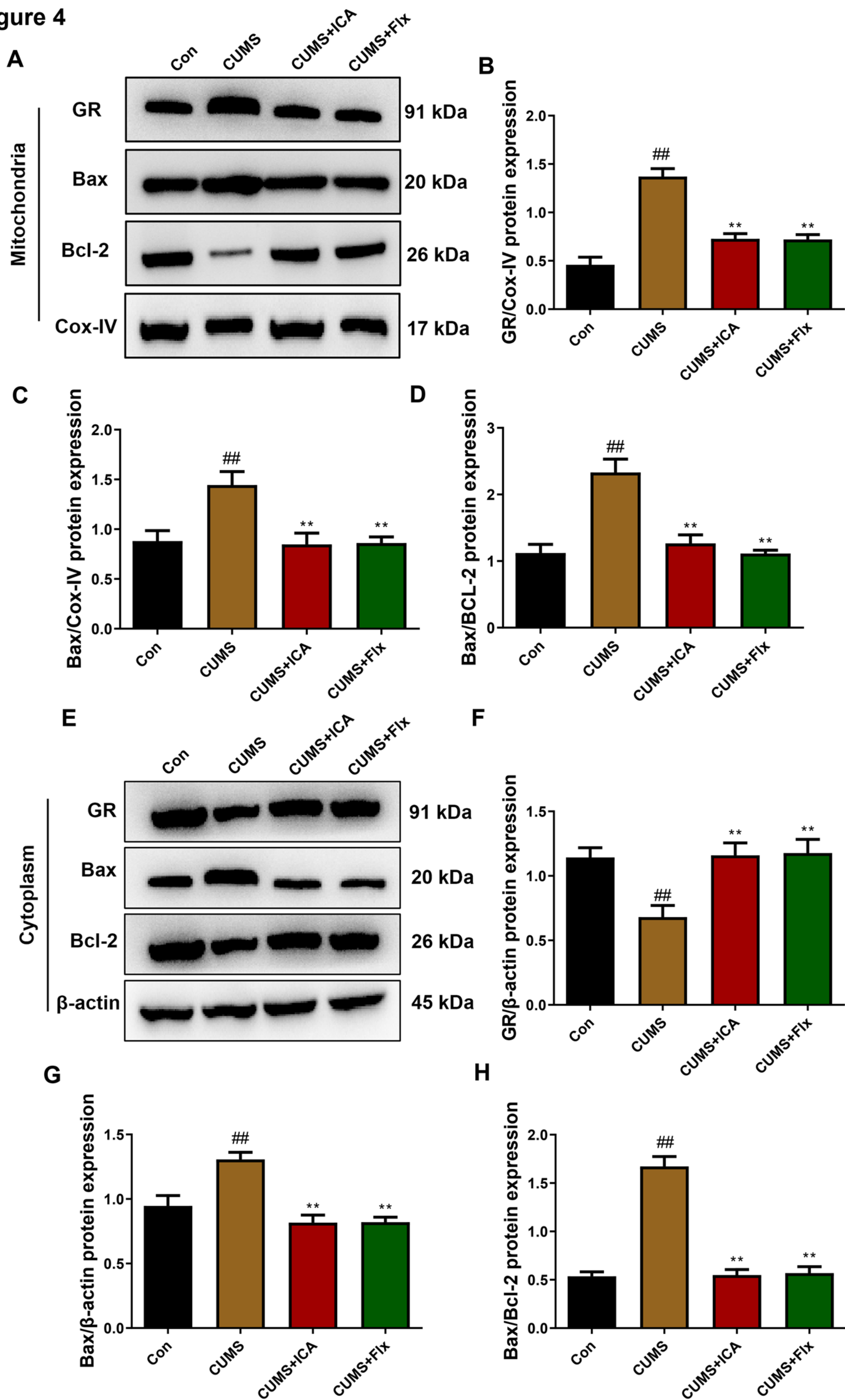

bioRxiv preprint doi: https://doi.org/10.1101/2023.03.09.531962; this version posted March 10, 2023. The copyright holder for this preprint (which was not certified by peer review) is the author/funder, who has granted bioRxiv a license to display the preprint in perpetuity. It is made available under aCC-BY 4.0 International license.

631 **Fig.4** Western blot experiment demonstrating the effect of icariin on mitochondrial and cytoplasmic GR,
632 Bcl-2 and Bax levels in rat hippocampus (A), (F)-(H) icariin treatment inhibited the expression of GR
633 and Bcl-2 of mitochondria in the CUMS hippocampus; (B), (C)-(E) The expression of GR, Bcl-2 and
634 Bax in cytoplasm. Data were presented as the mean + SD. ##P < 0.01 vs. Control group; *P < 0.05, **P
635 < 0.01 vs. CUMS group, df=11.

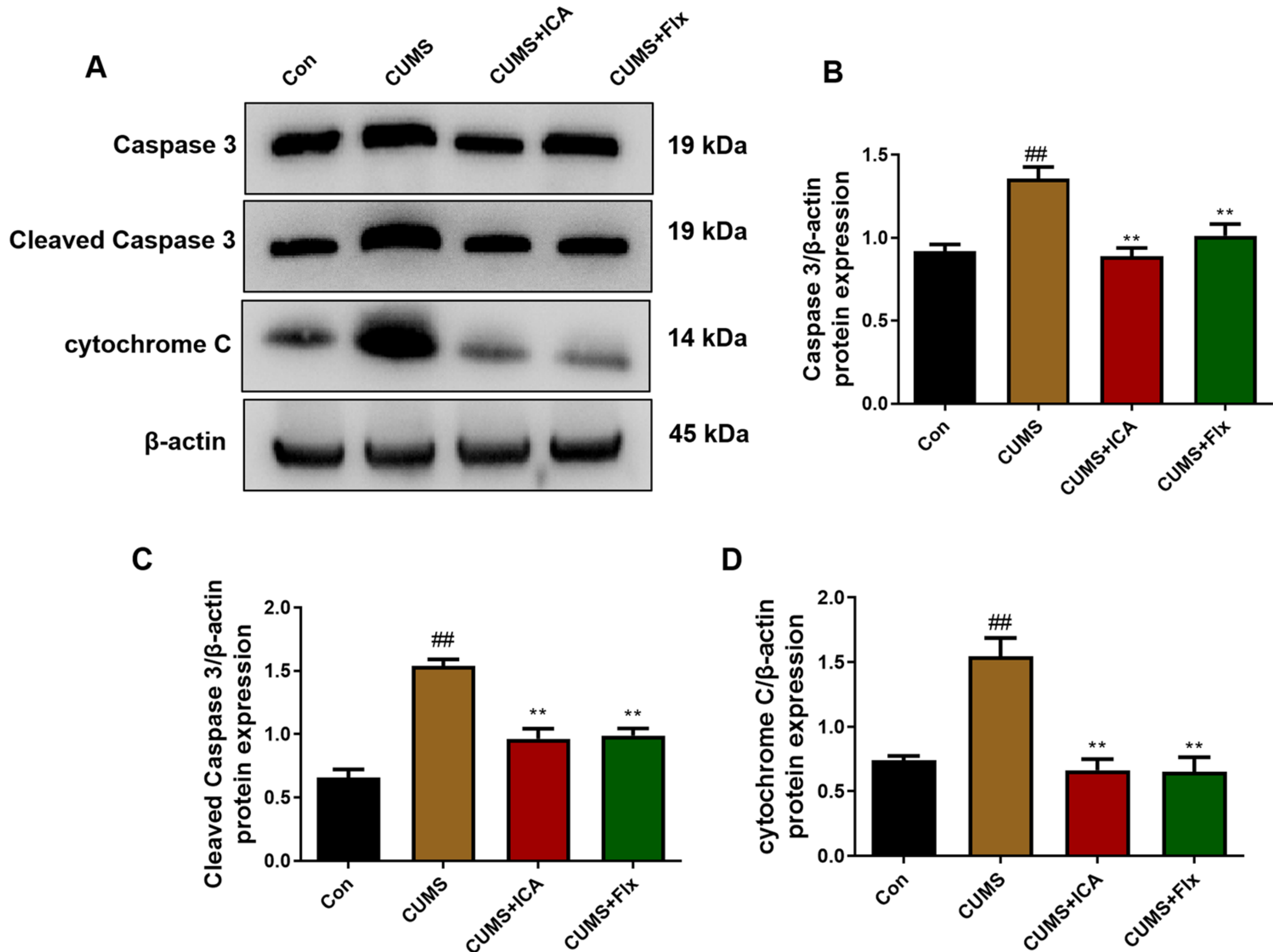

636

637 **Fig.5 ICA treatment effects on the expression of cytoplasmic apoptotic proteins.**
638 (A) Western blot was used to detected the apoptotic proteins (caspase 3 and cytochrome C) in
639 cytoplasmic. The bar graphs reflected the cleaved caspase 3 (B), caspase 3 (C), cytochrome C (D)
640 proteins expression in each group. Data were presented as the mean + SD. ##P < 0.01 vs. Control group;
641 *P < 0.05, **P < 0.01 vs. CUMS group, df=11.

642

bioRxiv preprint doi: https://doi.org/10.1101/2023.03.09.531962; this version posted March 10, 2023. The copyright holder for this preprint (which was not certified by peer review) is the author/funder, who has granted bioRxiv a license to display the preprint in perpetuity. It is made available under aCC-BY 4.0 International license.

Figure S1

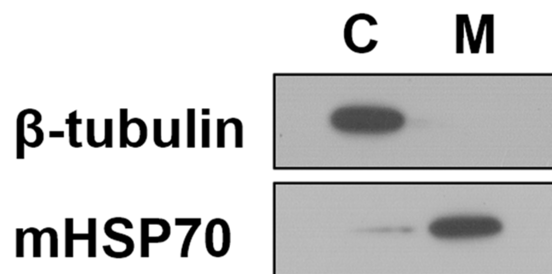

Fig.S1 The purity of subcellular fractions. The purity was assayed using specific antibodies against β-tubulin for cytoplasmic and mHsp70 for mitochondrial fraction.